Journal of Ovonic Research Vol. 8, No. 3, July - September 2012, p. 91 - 96

EFFECT OF UV ON IMPEDANCE SPECTROSCOPY OF Sn DOPED ZnO NANORODS

M. KASHIF[a*], SYED M. USMAN ALI[c], M. E. ALI[b], U. HASHIM[a]
[a]*Nano Biochip Research Group, Institute of Nano Electronic Engineering (INEE), Universiti Malaysia Perlis (UniMAP), 01000 Kangar, Perlis, Malaysia*
[b]*Nanotechnology and Catalysis Research Centre, Universiti Malaya, 50603 Kuala Lumpur, Malaysia*
[c]*Department of Electronic Engineering, NED University of Engineering and Technology, Karachi-75270, Pakistan*

Sn doped ZnO nanorods were grown on p-type silicon substrate using sol-gel method. Impedance spectroscopy of Sn doped ZnO nanorods were recorded under dark and UV conditions to study the frequency dependent electrical parameters such as impedance and conductivity for the Sn doped ZnO nanorods MSM structure in the range of 1 Hz to 10 MHz. The Nyquist plot of Sn doped ZnO nanorods showed two semicircle arcs that correspond to the distribution of the grain boundaries and electrode process. It was observed that with the exposure of UV light the 2nd semicircle arc that represents the electrode process is reduced. The conductivity plot revealed that the UV enhances the conduction of the Sn doped ZnO nanorods. SEM image showed the densily packed nanorods on the surface of silicon substrate, whereas XRD revealed that the grown nanorods have c-axis orientation.

(Received June 14, 2012; Accepted July 18, 2012)

Keywords: Sol-gel, Doping, Impedance, ZnO, UV

1. Introduction

Zinc oxide is an II–VI semiconductor with large band gap (E_g = 3.37 eV). It has a stable wurtzite structure with lattice spacing a = 0.325 nm and c = 0.521 nm. It has higher exciton binding energy (~60 meV). It is widely used in a number of applications like photo catalysis [1], gas sensors [2], varistors [3] and so on. Zinc oxide is non-toxic, and compatible with skin, making it a suitable additive for textiles and surfaces that come in contact with humans. It is also used as a catalyst for methanol synthesis. The electrical properties of ZnO originate from point native defects such as oxygen vacancies (V_o) and zinc interstitials (Z_{ni}^+) [4]. The electrical properties of nanomaterials are different from those of their bulk counter parts. The high surface-to-volume ratio of grains, small size, enhanced contribution from grains and grain boundaries, quantum confinement of charge carriers, band structure modification and defects in grains are some of the factors that contribute to the electrical properties of nanostructured materials [5]. The influence of grains and grain boundaries plays a crucial role in the transport properties, which can be investigated by impedance spectroscopy. Studies on the effect of UV source and frequency on the dielectric behaviour and impedance spectra of ZnO nanorods offer various informations about different polarization mechanisms, grain and grain boundary effect in nanostructured materials.

In this research, Sn doped ZnO nanorods were grown on p-type silicon substrate using low cost sol-gel method. For the fabrication and electrical characterization metal –semiconductor-metal configuration was employed by depositing circular silver electrodes on the top of Sn doped ZnO nanorods. The impedance characterstics of Sn doped ZnO nanorods as a photodetector under the exposure of 365 nm, 2mW UV light was investigated.

* Corresponding author: kashif_bme@yahoo.com ,

2. Experimental

Sn doped ZnO seed solution was prepared as reported elsewhere [6]. In short, zinc acetate dihydrate and stanium chloride were dissolved in 2-methoxyethanol, monoethanolamine was added dropwise in the solution as a stabilizer. The Sn/Zn ratio was 0.2wt% and the concentration of the solution was maintained at 0.35M. Sn doped ZnO seed solution was coated on p-type silicon substrate using spin coater at 3000 rpm for 30 sec. The sample was dried at 60ºC followed by baking at 250ºC for 15 minutes in order to dry the film and vaporize the organic solvents. The coating to drying process was repeated five times. Finally the film was annealed at 500ºC for 2 hrs under atmospheric conditions. After growth, the subsrate was immersed in the growth solution. The growth solution was prepared by dissolving zinc nitrate hexahydrate, hexamethyltetramine in DI water. The overall concentration of the growth solution was 0.025M. The solution was stirred for 4 hours in order to get good mixing. After that, the sample was incubated in a preheated oven and the preheating temperature was set to 93ºC . The sample was inserted inside the growth solution and was holded with teflon sample holder with film coated side faced down inside the growth solution. The incubation time for the growth was 5 hrs and after that the oven was ramp down to room temperature. The sample was taken out from the growth solution at room temperature and washed with DI water for 2-3 times in order to remove the powder. At the end the circular silver electrodes were deposited on the top of ZnO nanorods using Auto306 vaccum thermal evaporator.

The crystalinity of the Sn doped ZnO nanorods was measured using Bruke D8 x-ray diffraction with a CuKα radiation source of (λ=1.5406Å). The topography and morphology of the Sn doped ZnO nanorods were observed using scanning electron microscope (JEOL JSM 6460 LA). For the electrical characterization circular silver electrodes were deposited on the top of Sn doped ZnO nanorods using hard mask. The electrical measurement was performed using alpha high dielectric analyzer from Novacontrol in the frequency range of 1Hz – 10MHz at room temperature.

3. Results and discussion

Fig. 1 shows the SEM images of the Sn doped ZnO nanorods. It was observed that the nanorods are perpendicular to the substrate and the silicon substrate is fully packed with high density Sn doped ZnO nanorods. The average diameter of the nanorods was within the range of 60-100nm.

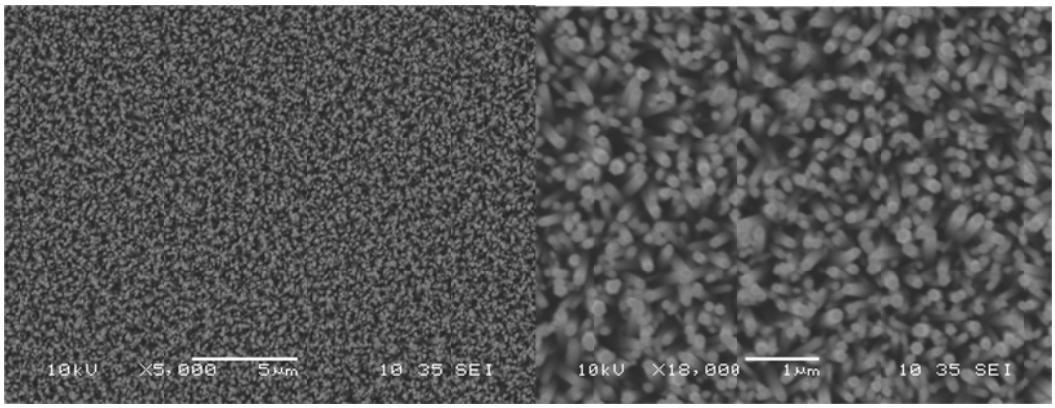

Fig. 1. SEM image of 0.2wt% Sn doped ZnO nanorods.

Fig. 2 shows the XRD pattern of Sn doped ZnO nanorods. Several peaks were observed at 002 (34.348˚), 101(36.32˚), 102 (47.606˚), 103(62.89˚), showing a good agreement with the ZnO

JCPDs card 36-1451. The high intensity of 002 peaks corresponds to a better crystallinity of ZnO which had a c-axis orientation. No peaks other than ZnO were observed, reflecting the purity of the fabricated Sn doped ZnO nanorods.

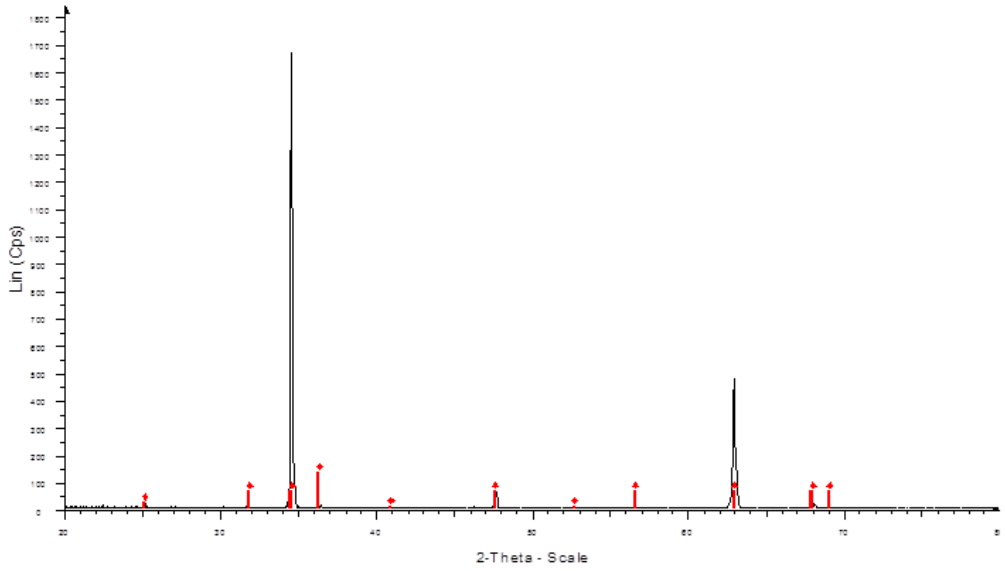

Fig. 2. XRD pattern of 0.2%wt Sn doped ZnO nanorods

AC impedance spectroscopy has been proven a powerful method to estimate the contribution of the grain, grain boundaries and film-electrode effects on the charge transport phenomenon [7]. The complex impedance as a function of angular frequency (ω) can be represented by the following equation [8]:

$$Z^*(\omega) = Z'(\omega) - jZ''(\omega) \quad (1)$$

Where Z'(ω) and Z"(ω) are the real and imaginary components of the complex impedance, respectively. For the polycrystalline material, the total impedance Z_T can be written as [9]:

$$Z_T = Z_g + Z_{gb} + Z_c \quad (2)$$

Where Z_g, Z_{gb} and Z_c represent the complex impedance contribution of the grains, grain boundaries, and electrode contact, respectively.

Figure 3(a,b) shows the variation of the real (Z') and imaginary (Z") components of the impedance with frequency. The magnitude of both the components decreased when the frequency increased, indicating an increase in AC conductivity of the nanorods. The real and imaginary components of Sn doped ZnO nanorods decreased with the exposure of UV light, reflecting that the structure is more conductive as compared to dark conditions.

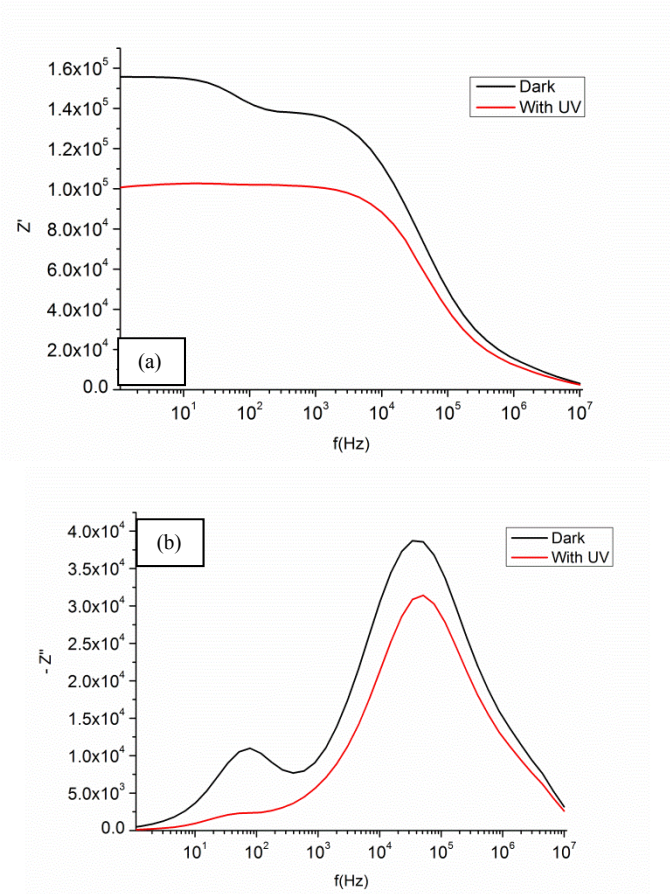

Fig. 3(a) Frequency versus Z' for Sn doped ZnO nanorods, and (b) Frequency versus Z'' for ZnO nanorods at room temperature under dark and UV conditions

Fig. 4 shows the Nyquist plot of Sn doped ZnO nanorods. The plot shows a semicircle arc at higher frequency corresponding to the electrical properties of grain boundaries. Whereas, at low frequencies, the plot shows a depress semicircle that corresponds to the nanorods/electrode interface contribution due to the polarization mechanism in this range of frequencies. With the exposure of UV light the 2nd arc becomes less prominent because of the excitation of electrons from conduction band to valence band. The UV exposure reduces the band gap and electrons can transport easily as compared to dark conditions. The previous researchers reported [10] the presence of 2nd semicircle under biased conditions. They relate the appearance of the arc to the accumulation of adsorbed oxygen molecules at the film-electrode contact area. As in our case the arc appeared at zero bias volts which were believed to be due to the holes trapped at the contact area. The high resistance component at the leftmost region was the high frequency region representing the effect of grain and grain boundary components, while the low resistance value at the rightmost region namely low frequency region reflects the effect of metal-semiconductor contact.

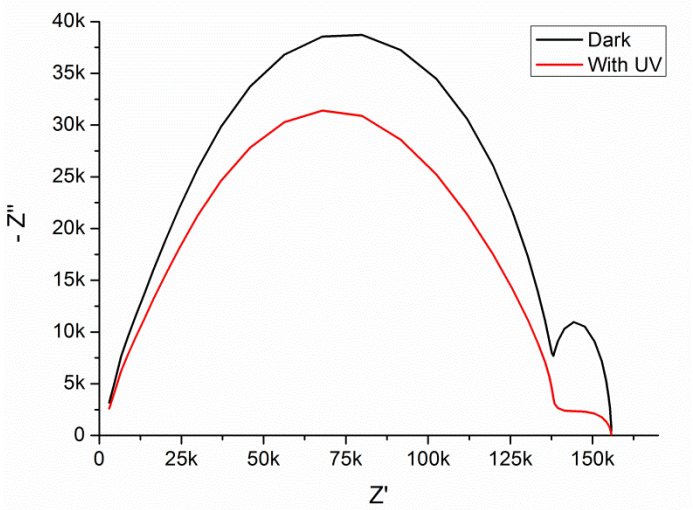

Fig. 4. Nyquist plot for 0.2wt% Sn doped ZnO nanorods under dark and UV conditions

Fig. 5 shows the electrical conductivity curve of Sn doped ZnO nanorods under dark and UV conditions. At the applied frequency range of 10 KHz- 10 MHz as shown in inset of figure 5, the conductivity follows the Jonscher power law relation [11]:

$$\sigma = A\omega^s \tag{3}$$

Where ω is the angular frequency, A is a constant and the exponent s is a frequency dependent parameter having values less than unity [12]. The electrical conductivity increases with the exposure of UV light.

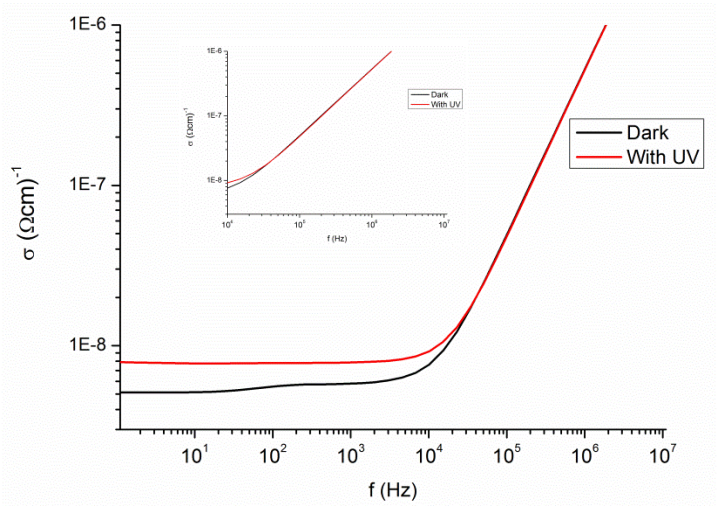

Fig. 5. Ac conductivity (σ) as a function of frequency for 0.2wt% Sn doped ZnO nanorods under dark and UV conditions

4. Conclusion

Sn doped ZnO nanorods were successfully synthesized using low cost sol-gel method. Highly populated and vertical aligned Sn doped ZnO nanorods were observed from the SEM images. The XRD pattern shows the preferred c-axis orientation of Sn doped ZnO nanorods. The electrical parameters like impedance and ac conductivity as a function of frequency were studied for the grown ZnO nanorods in the frequency range of 1Hz -10 MHz. The impedance plane shows two regions corresponding to grain boundaries and grain boundaries-electrodes process. Under the

exposure of UV light the real and imaginary components of impedance decreased whereas the conductivity increased that revealed that the UV source excites the electrons so that they can jump from valance band to electron band.

Acknowledgements

The author would like to acknowledge the financial support for the FRGS grant number (9003-00276) from ministry of higher education (MOHE). The author would also like to thank to the technical staff of Institute of Nano Electronic Engineering and School of Microelectronic Engineering, University Malaysia Perlis for their kind support to smoothly perform the research.

References

[1] Y. Liu, Z. H. Kang, Z. H. Chen, I. Shafiq, J. A. Zapien, I. Bello, W. J. Zhang, and S. T. Lee, Cryst. Growth Des. 9, 3222 (2009).
[2] Y.-Z. Lv, C. -R. Li, L. Guo, F. -C. Wang, Y. Xu, and X.-F. Chu, Sens. Actuators B. **141**, 85 (2009).
[3] B.-H. Lee and S.-M. Kang, Curr. Appl. Phys. **6**, 844 (2006).
[4] S. Lany and A. Zunger, Phys. Rev. Lett. **98**, 045501(2007).
[5] V. Biju and M. Abdul Khadar, J. Mater. Sci. **36**, 5779 (2001).
[6] M. Kashif, U. Hashim, S. M. Usman Ali, M. Willander, and M. Ibrar-ul-Haque, presented at the Multitopic Conference (INMIC), 2011 IEEE 14th International, Dec 22-24-th Dec. 2011, Karachi, Pakistan.
[7] Syed Mahboob, G. Prasad, and G. Kumar, Bull. Mater. Sci. 29, 347 (2006).
[8] M. Abdullah and A. Yusoff, J. Mater. Sci. 32, 5817 (1997).
[9] N. H. Al-Hardan, M. J. Abdullah, H. Ahmad, A. Abdul Aziz, and L. Y. Low, Solid State Electron. **55**, 59 (2011).
[10] Yongki Min, Harry L. Tuller, Stefan Palzer, Jürgen Wöllenstein, and Harald Böttner, Sens. Actuators B. **93**, 435 (2003).
[11] M. K. Gupta, N. Sinha, B. K. Singh, N. Singh, K. Kumar, and Binay Kumar, Mater. Lett. **63**, 1910 (2009).
[12] AK Jonscher, Dielectric relaxation in solids, London: Chelsea Dielectric Press (1983).